Particle Accelerators
1984 Vol. 14 pp. 185-199
0031-2460/84/1403/0185$18.50/0

ON COMPENSATION OF AXIAL ELECTRIC FIELD UNFLATNESS IN MULTICELL ACCELERATING STRUCTURES†

P. FERNANDES

Istituto per la Matematica Applicata del CNR, Genova, Italy

and

R. PARODI

INFN, Sezione di Genova, Genova, Italy

(*Received April 29, 1983*)

We propose a lumped-parameter equivalent circuit for a TM_{01} multicell standing-wave accelerating structure with full end cells. With the suggested model, we can compute the amount of end-cell frequency compensation needed to achieve field flatness in the highest mode of the structure. We also show that the same compensation works as well for structures with beam tubes, provided its length is at least twice its radius. An application to a five-cell superconducting structure is reported.

1. INTRODUCTION

A multicell TM_{01} structure is often operated in the highest TM_{01} band-pass resonant mode, which is the most efficient one for accelerating devices since it has the highest shunt impedance.[1] But, if all the cells of the structure are equal to each other, field flatness cannot be obtained in this mode in a real accelerating structure with beam tubes in the end cells. That is to say, we cannot achieve equal peak intensity of the axial electric field in each cell. Now if we can get field flatness by slight geometrical corrections of some cells, several advantages follow: a) efficiency is still improved by a higher shunt impedance; b) peak surface fields are lowered, thus increasing the accelerating field achievable in superconducting structures before electron loading or superconductivity breakdown takes place, and c) field asymmetry in cavities, which may cause multipacting,[2] is reduced.

In the present paper, which extends a previous internal report,[3] we develop a method to compute the end-cell correction needed to compensate unflatness in the highest TM_{01} mode of a multicell structure. The amount of correction can be calculated knowing only the 0 and π mode frequencies of a single cell of the structure, which are readily found by using computer codes like LALA or SUPERFISH.[4,5] The aforesaid method is founded on a model which coincides with that proposed by E. Haebel and J. Tuckmantel[6] for tuning of multicell structures.

† Work supported in part by CERN.

2. EQUIVALENT CIRCUIT

Many papers[7-10] deal with lumped-constant equivalent circuits for multicell structure, but only a few[9,10] report about models with full end cells; most of the authors in fact treat only the problem of a structure with half end cells. Those papers in which a model for structures with full end cells is reported are, in our opinion, unsatisfactory since the solution of the model equations is carried out only for one type of boundary conditions at the irises of the end cells.

The model shown in Fig. 1, corresponding to the lumped circuit of a *TM* waveguide,[11] is suggested by us as an equivalent circuit of a structure with an infinite number of equal cells coupled through the *E*-field, each cell being represented by an *LC* resonator and the coupling by a capacitor C_K. Taking the Fourier transform of the differential equation for the m-th resonator, we get

$$\left(j\omega L + \frac{1}{j\omega}\left(\frac{1}{C} + \frac{2}{C_K}\right)\right) i_m = \frac{1}{j\omega C_K}(i_{m-m} + i_{m+1}) \tag{1}$$

from which we obtain the dispersion relation of this infinite structure model as

$$\omega_\Phi{}^2 = \frac{1}{LC} + \frac{2}{LC_K}(1 - \cos \Phi), \tag{2}$$

where Φ is the phase shift of the current between contiguous resonators.

Now let us consider a section of N coupled resonators of the infinite chain in the proposed model (Fig. 1, resonators from 1 to N). This section can be regarded as independent from the rest of the chain provided there is no coupling between resonators 0, 1 and resonators N, $N + 1$. With this assumption, we will find the normal modes frequencies of the above-mentioned section.

Assuming no coupling between resonators 0 and 1, only the following relations connecting together the currents i_0 and i_1 are allowed

(a) $$i_0 = i_1 \tag{3}$$

(b) $$i_0 = -i_1 \tag{4}$$

The equation for i_1 becomes

$$\left(j\omega L + \frac{1}{j\omega}\left(\frac{1}{C} + \frac{1}{C_K}\right)\right) i_1 = \frac{1}{j\omega C_K} i_2 \tag{5}$$

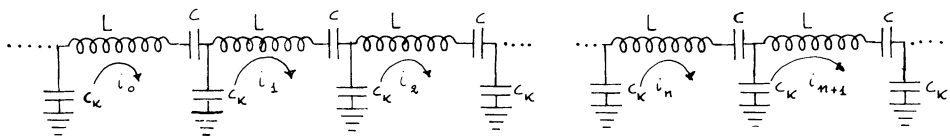

FIGURE 1 Lumped-constant model of an infinite structure.

by condition (3) and

$$\left(j\omega L + \frac{1}{j\omega}\left(\frac{1}{C} + \frac{3}{C_K}\right)\right) i_1 = \frac{1}{j\omega C_K} i_2 \tag{6}$$

by condition (4).
A similar argument holds at the other end of the section.

Thus the linear algebraic system solving the problem of finding normal modes with conditions like (3) at both ends is

$$\begin{cases} \left(j\omega L + \dfrac{1}{j\omega}\left(\dfrac{1}{C} + \dfrac{1}{C_K}\right)\right) i_1 - \dfrac{1}{j\omega C_K} i_2 = 0 \\ -\dfrac{1}{j\omega C_K} i_1 + \left(j\omega L + \dfrac{1}{j\omega}\left(\dfrac{1}{C} + \dfrac{2}{C_K}\right)\right) i_2 - \dfrac{1}{j\omega C_K} i_3 = 0 \\ \qquad\qquad \cdots\cdots \\ -\dfrac{1}{j\omega C_K} i_{N-2} + \left(j\omega L + \dfrac{1}{j\omega}\left(\dfrac{1}{C} + \dfrac{2}{C_K}\right)\right) i_{N-1} - \dfrac{1}{j\omega C_K} i_N = 0 \\ -\dfrac{1}{j\omega C_K} i_{N-1} + \left(j\omega L + \dfrac{1}{j\omega}\left(\dfrac{1}{C} + \dfrac{1}{C_K}\right)\right) i_N = 0, \end{cases} \tag{7}$$

whereas for conditions like (4) we have

$$\begin{cases} \left(j\omega L + \dfrac{1}{j\omega}\left(\dfrac{1}{C} + \dfrac{3}{C_K}\right)\right) i_1 - \dfrac{1}{j\omega C_K} i_2 = 0 \\ -\dfrac{1}{j\omega C_K} i_1 + \left(j\omega L + \dfrac{1}{j\omega}\left(\dfrac{1}{C} + \dfrac{2}{C_K}\right)\right) i_2 - \dfrac{1}{j\omega C_K} i_3 = 0 \\ \qquad\qquad \cdots\cdots \\ -\dfrac{1}{j\omega C_K} i_{N-2} + \left(j\omega L + \dfrac{1}{j\omega}\left(\dfrac{1}{C} + \dfrac{2}{C_K}\right)\right) i_{N-1} - \dfrac{1}{j\omega C_K} i_N = 0 \\ -\dfrac{1}{j\omega C_K} i_{N-1} + \left(j\omega L + \dfrac{1}{j\omega}\left(\dfrac{1}{C} + \dfrac{3}{C_K}\right)\right) i_N = 0 \end{cases} \tag{8}$$

These linear systems, written in matrix form, become respectively

$$\begin{pmatrix} (\alpha - 1) & -1 & 0 & 0 & \cdot & \cdot & \cdot \\ -1 & \alpha & -1 & 0 & \cdot & \cdot & \cdot \\ 0 & -1 & \alpha & -1 & \cdot & \cdot & \cdot \\ \cdot & \cdot & \cdot & \cdot & \cdot & -1 & 0 \\ \cdot & \cdot & \cdot & \cdot & \cdot & \alpha & -1 \\ 0 & 0 & 0 & \cdot & 0 & -1 & (\alpha - 1) \end{pmatrix} \begin{pmatrix} i_1 \\ i_2 \\ \cdot \\ \cdot \\ \cdot \\ i_N \end{pmatrix} = 0 \tag{9}$$

$$\begin{pmatrix} (\alpha+1) & -1 & 0 & 0 & \cdot & \cdot & \cdot \\ -1 & \alpha & -1 & 0 & \cdot & \cdot & \cdot \\ 0 & -1 & \alpha & -1 & \cdot & \cdot & \cdot \\ \cdot & \cdot & \cdot & \cdot & \cdot & -1 & 0 \\ \cdot & \cdot & \cdot & \cdot & \cdot & \alpha & -1 \\ 0 & 0 & 0 & \cdot & 0 & -1 & (\alpha+1) \end{pmatrix} \begin{pmatrix} i_1 \\ i_2 \\ \cdot \\ \cdot \\ \cdot \\ i_N \end{pmatrix} = 0 \tag{10}$$

where

$$\alpha = 2 + \frac{C_K}{C} - \omega^2 L C_K = 2\cos\Phi \tag{11}$$

Thus we have reduced the problem to one of computing the eigenvalues of a matrix. By solving the characteristic equations, we obtain the roots corresponding to the phase shift per resonator

$$\Phi = \frac{K-1}{N}\pi \qquad K = 1, \ldots, N \tag{12}$$

from (9) and

$$\Phi = \frac{K}{N}\pi \qquad K = 1, \ldots, N \tag{13}$$

from (10).

The eigenvector belonging to an eigenvalue is the resonator current in the corresponding mode.

With the lowest eigenvalue of (9), we find equal currents in all the resonators, whilst with the highest eigenvalue of (10), we find currents of equal intensity but with sign changing from one resonator to the next.

Our results (12) agree with those obtained by *W.* Bauer[10] using a different model but with conditions equivalent to (3).

For the sake of completeness, by imposing the conditions

$$i_0 = i_2 \qquad i_{N-1} = i_{N+1}, \tag{14}$$

we fit our model to a structure with an electric mirror in the centers of the first and last cells in a way similar to that proposed by Bauer for his model. The corresponding system is

$$\begin{pmatrix} \alpha/2 & -1 & 0 & 0 & \cdot & \cdot & \cdot & \cdot \\ -1 & \alpha & -1 & 0 & \cdot & \cdot & \cdot & \cdot \\ 0 & -1 & \alpha & -1 & \cdot & \cdot & \cdot & \cdot \\ \cdot & \cdot & \cdot & \cdot & -1 & \alpha & -1 & 0 \\ \cdot & \cdot & \cdot & \cdot & 0 & -1 & \alpha & -1 \\ \cdot & \cdot & \cdot & \cdot & 0 & 0 & -1 & \alpha/2 \end{pmatrix} \begin{pmatrix} i_1 \\ i_2 \\ \cdot \\ \cdot \\ \cdot \\ i_N \end{pmatrix} = 0 \tag{15}$$

The eigenvalues found by solving the characteristic equation correspond to the modes with phase shift per resonator

$$\Phi = \frac{K-1}{N-1}\pi \qquad K = 1, \ldots, N \tag{16}$$

3. FIELD DISTRIBUTION IN THE CELLS OF THE STRUCTURE

The solution of the eigenvalue problem for the lumped-constant equivalent circuit also gives some useful information on the field distribution in the structure.

In fact the eigenvector giving, as already mentioned, the resonator currents in the model, also gives the relative amplitude of the electric field in the different cells of the structure. Thus, starting from a given multicell structure and its boundary conditions, it is possible to predict the field unflatness in the different modes and the amount of correction required to achieve the goal of field flatness in the highest mode. In the following example, we restrict ourselves to deal with a 3-cell structure.

If we impose electric-mirror conditions at the irises of the end cells (corresponding for the lumped model to conditions like (3)) we get in the highest mode of the structure (the $2\pi/3$ mode) the eigenvector $(1, -2, 1)$. Thus, in the $2\pi/3$ mode, the intensity of the electric field in the central cell of the structure is twice that in any end cell.

If we impose in the lumped model conditions like (4) (i.e. magnetic mirror at the irises of the end cells of the structure), we get in the highest mode of the structure (the π mode) a thoroughly flat field distribution, the eigenvector being $(1, -1, 1)$.

4. END CELLS COMPENSATION OF A STRUCTURE WITH FULL END CELLS TERMINATED BY METAL PLATES

We now discuss a method to achieve field flatness in a finite multicell standing-wave structure with full end cells terminated by metal plates. Such a structure, of course, cannot be used as an accelerating device; nevertheless the method of compensation developed for it will turn out to work also for structures with beam tubes, as we propose to show in section 5.

In a finite multicell standing-wave structure, magnetic mirror boundary conditions on the irises of the end cells are not allowed and it is only possible to have electric-mirror conditions when the first and last irises are closed by metal plates.

For this reason, if all the cells of the structure are identical, it is impossible to achieve field flatness in the highest mode. A certain amount of compensation is needed in the structure to achieve the goal of a field with equal amplitude in each cell. The way to compute this amount of compensation is straightforward and comes out by inspection of the lumped-constant models of the conditions (3) and (4) shown in Fig. 2.

To establish the correctness of these models, we observe that the condition (3) is equivalent to replace the coupling capacitor C_K between the 0 and 1 resonators of the infinite chain (see Fig. 1) by a short-circuit, while the condition (4) is equivalent to splitting the capacitor in two equal parts between the two contiguous resonators taking into account, for the 1 resonator, the i_1 current only. We also remark that the difference between the models for the boundary conditions is only the $C_K/2$ capacitor.

Now if in a multicell structure the end cells are modified in such a way that they have the slightly different resonant frequency resulting by adding in the model a $C_K/2$ series

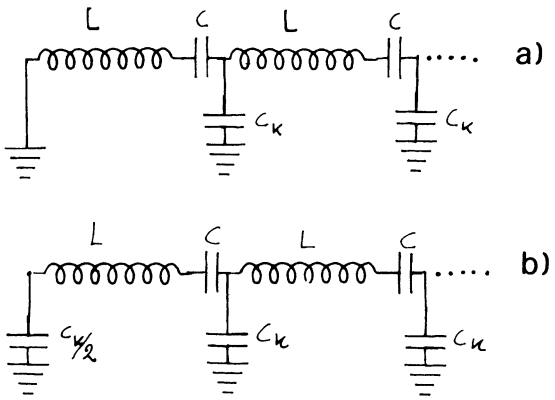

FIGURE 2 Lumped-constant model of: (a) condition (3); (b) condition (4).

capacitor in each end resonator, the field flatness needed can be achieved. As a matter of fact, for a multicell structure with electric-mirror boundary conditions at the end cells, but with the end-cell compensation explained above, the model is identical to the one for the same structure with magnetic-mirror boundary conditions and no end-cell compensation.

Thus we get, of course, the same equations and the same solutions for both cases and so, in the highest mode of the compensated structure, we have the required field flatness.

Given a multicell structure, the values of L, C and C_K in the corresponding model are not known and, for compensating the end cells, some computations are needed to express them as a function of the known parameters of the structure.

From the dispersion relation (2) we get

$$\omega_\pi^2 - \omega_0^2 = \frac{4}{LC_K}; \tag{17}$$

the coupling coefficient K (or fractional bandwidth) is by definition

$$K = 2\frac{\omega_\pi - \omega_0}{\omega_\pi + \omega_0} \tag{18}$$

From Eqs. (17) and (18) it is straightforward to obtain, by some amount of algebra, the ratio C/C_K as a function of K. In fact for coupling coefficients of a few percent, we can approximate ω_π by ω_0 and write

$$K = 2\frac{\omega_\pi^2 - \omega_0^2}{(\omega_\pi + \omega_0)^2} \simeq 2\frac{\omega_\pi^2 - \omega_0^2}{4\omega_0^2}; \tag{19}$$

now substituting (17) and

$$\omega_0^2 = \frac{1}{LC} \tag{20}$$

(again obtained from Eq. (2)) in Eq. (19), we find

$$K \simeq 2\frac{\frac{4}{LC_K}}{\frac{4}{LC}} \tag{21}$$

from which

$$\frac{C}{C_K} \simeq \frac{K}{2}. \tag{22}$$

We can now compute the frequency of the compensated cell. By inspection of the model, the new frequency of the first cell must be

$$\omega_C{}^2 = \frac{1}{L\left(\frac{1}{\frac{1}{C} + \frac{2}{C_K}}\right)} = \frac{1}{LC\left(\frac{1}{1 + \frac{2C}{C_K}}\right)} = \frac{1}{LC}\left(1 + \frac{2C}{C_K}\right) \simeq \omega_U{}^2(1 + K) \tag{23}$$

or

$$\omega_C \approx \omega_U\sqrt{1 + K} \approx \omega_U\left(1 + \frac{K}{2}\right), \tag{24}$$

where

$$\omega_U = \frac{1}{LC} = \omega_0 \tag{25}$$

is the frequency of the uncompensated cell. This result again agrees with the corresponding one reported by Bauer.[10]

It should be noted that Eq. (24) expresses the frequency-correction factor for the end cell only in terms of the fractional bandwidth of the corresponding infinite structure, which can be easily calculated by a simulation code for resonant cavity like LALA[4] *or SUPERFISH.*[5] To compute K, we must substitute in (18) the 0 mode and π mode frequencies of the infinite structure as obtained by simulating a single cell of the structure with Neumann and Dirichelet boundary conditions, respectively, on the iris planes.

Incidentally, we remark that also the dispersion relation (2) can be rewritten in terms of these same frequencies as

$$\omega_\Phi{}^2 = \omega_0{}^2 + \frac{1}{2}(\omega_\pi{}^2 - \omega_0{}^2)(1 - \cos\Phi) \tag{26}$$

and used, together with (12) and (13), for calculating the resonant frequencies of a finite structure.

TABLE I

Highest mode resonant frequencies of some three-cell structures obtained by (a) the proposed model and (b) numerical simulation

	lumped-constant model		LALAGE
	frequency[a] (MHz)	currents	frequency (MHz)
Uncompensated with electric mirror	4242.86	(1, −2, 1)	4249.42
Uncompensated with magnetic mirror	4260.69	(1, −1, 1)	4257.47
Compensated with electric mirror	4260.69	(1, −1, 1)	4259.00

[a] From (26) with $\omega_0^2 = 6.9273\ 10^{20}\ \text{sec}^{-2}$ and $\omega_\pi^2 = 7.1667\ 10^{20}\ \text{sec}^{-2}$ obtained by LALAGE in single-cell simulation.

To check the predictions relying upon our simple model, we used the LALAGE code[12,13] to compute the highest-mode field distribution and resonant frequency of a three-cell TM_{01} structure. The boundary conditions at the irises of the end cells were Neumann conditions, or electric mirror, corresponding in the lumped-constant model to conditions like (3).

The frequency so obtained agrees within 0.1% with the $2\pi/3$ mode frequency calculated from the dispersion relation (26) (see Table I). Moreover from Fig. 3,

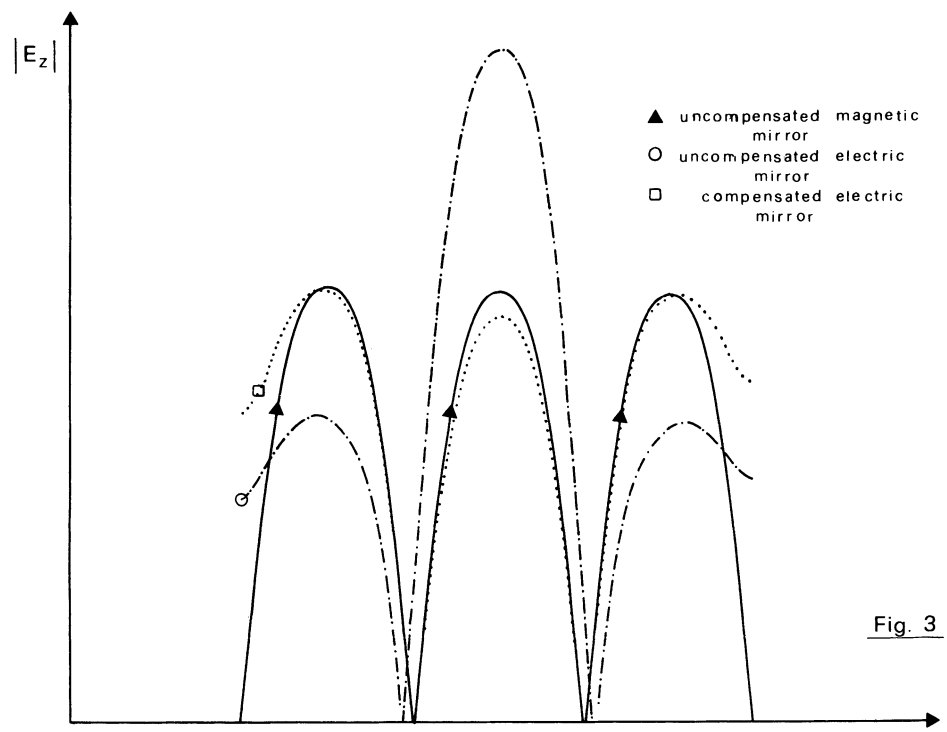

FIGURE 3 Highest mode electric field on axis (absolute value) for some three-cell structures terminated by metal plates as computed by LALAGE.

showing the electric field distribution as computed by the LALAGE code, and Table I it can be seen that the peak fields in the different cells are in the same ratio as the $2\pi/3$ mode currents in corresponding resonators of the lumped-parameter equivalent circuit (see also section 3).

Next equations (18) and (24) were used for calculating the amount of compensation needed to achieve the field flatness in the highest mode; we found that the end cells of the structure must be 0.86% higher in frequency than the central cell. This compensation leads to a 0.24-mm reduction of the end-cell radius, from $\Delta r/r \simeq \Delta\omega/\omega$.

To simulate a compensated structure with the same boundary conditions as above, we again ran the LALAGE program, obtaining a 4259-MHz highest-mode resonant frequency and a field distribution, by inspection of which it can be readily seen that the goal of field flatness is achieved (see Fig. 3).

As a last check, we again simulated the uncompensated structure but with magnetic-mirror boundary conditions at the irises; we obtained, as expected, a thoroughly flat field distribution and a resonant frequency in good agreement with: (a) the one previously found for the compensated structure and (b) the mode frequency computed from (26) (see Fig. 3 and Table I).

These results confirm the accuracy of our assumptions for the end-cell compensation of a structure terminated by metal plates in the highest mode of the TM_{01} band-pass.

5. END-CELL COMPENSATION OF AN ACCELERATING STRUCTURE WITH BEAM TUBES

In a real standing-wave accelerating structure, the situation of an end cell does not correspond to either conditions (3) or (4) since it is perturbed by a tube, starting at the iris plane, for beam injection or extraction. We can simulate this beam tube in the lumped-constant model by a shunt capacitor of unknown value C_B (see Fig. 4) such that

$$\frac{C_K}{2} < C_B < \infty, \tag{27}$$

the lowest value being used when the beam tube has zero length and the infinite value when the tube has infinite length. This assumption is reasonable in our opinion, since when the tube has zero length the lines of the electric field end on the iris with a field layout very similar to the magnetic-mirror boundary conditions and when the tube has infinite length, they intersect the iris plane almost perpendicularly as when electric-mirror boundary conditions are imposed. Indeed the suggested model for end cells with beam tubes leads to resonant frequencies of the whole structure that lie between the

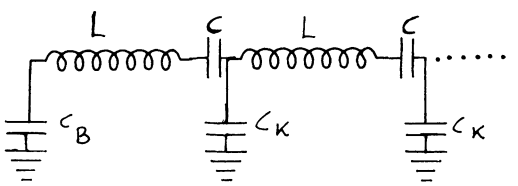

FIGURE 4 Lumped-constant model of an end cell with beam tube.

extreme values ω_0 and ω_π. In particular, when

$$C_B = \frac{C_K}{2}, \tag{28}$$

the highest mode frequency is equal to ω_π and when

$$C_B = \infty, \tag{29}$$

the lowest frequency is equal to ω_0.

But when dealing with a practical superconducting structure, the beam tubes must be long enough to prevent excessive power loss in their normal sections. Now, since a beam tube is a circular waveguide operated below the cutoff frequency, the ratio between its length d and its radius a must be about 3 to obtain a 60-db attenuation (a reasonable one).

Our measurements and computer simulations show that already for lower ratios d/a, the electric-field distributions agree fairly well with those of an identical structure with beam tubes replaced by metal plates closing the irises. In Figs. 5 and 6, we show as an

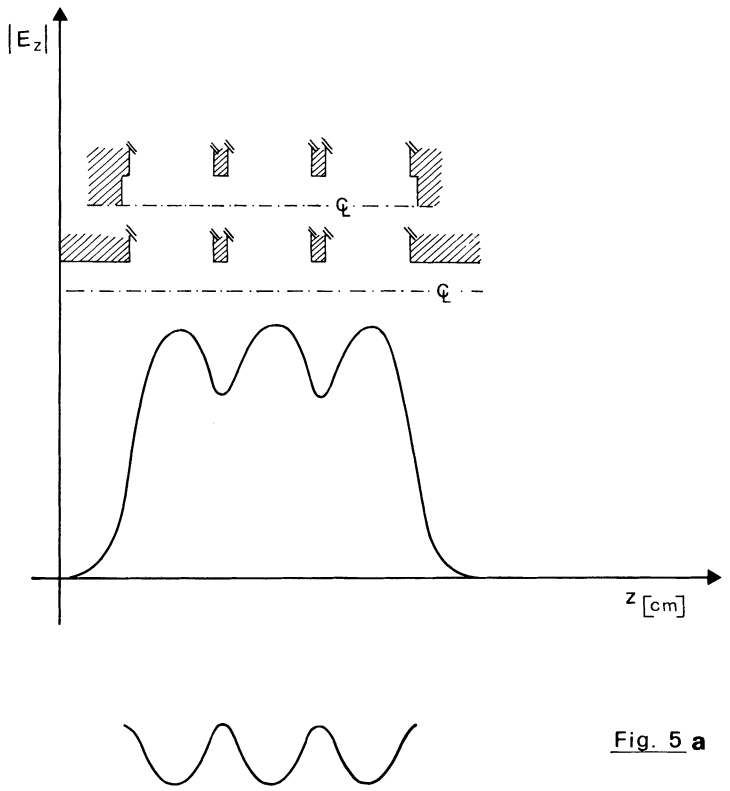

FIGURE 5 Computed axial electric field (absolute value) in a three-cell structure with beam tubes (d/a = 2.25) and with metal disk: (a) 0 mode, (b) $\pi/3$ mode, (c) $2\pi/3$ mode (for the graphs concerning the metal disk case the $|E_z|$ axis is reversed).

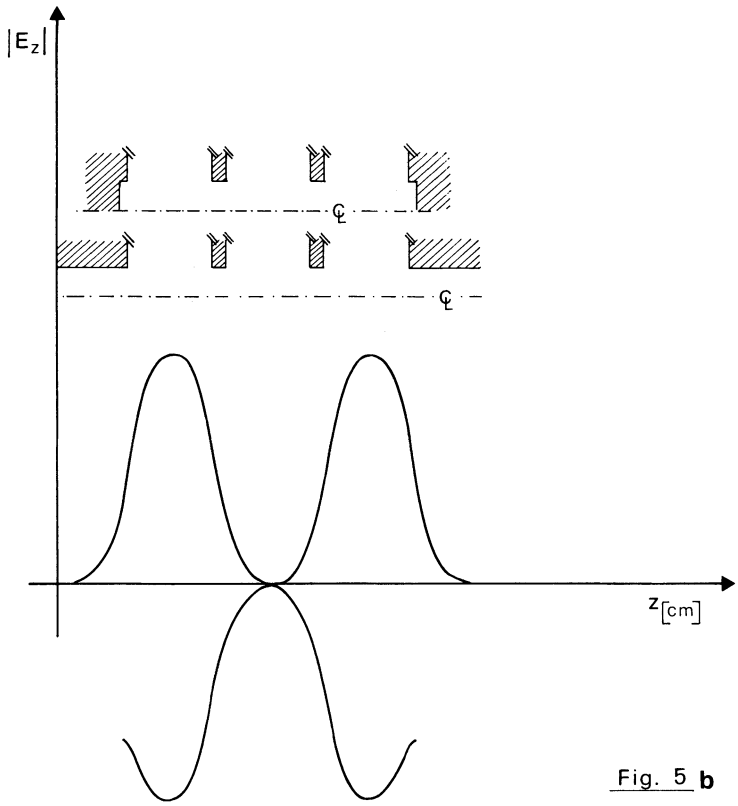

Fig. 5 b

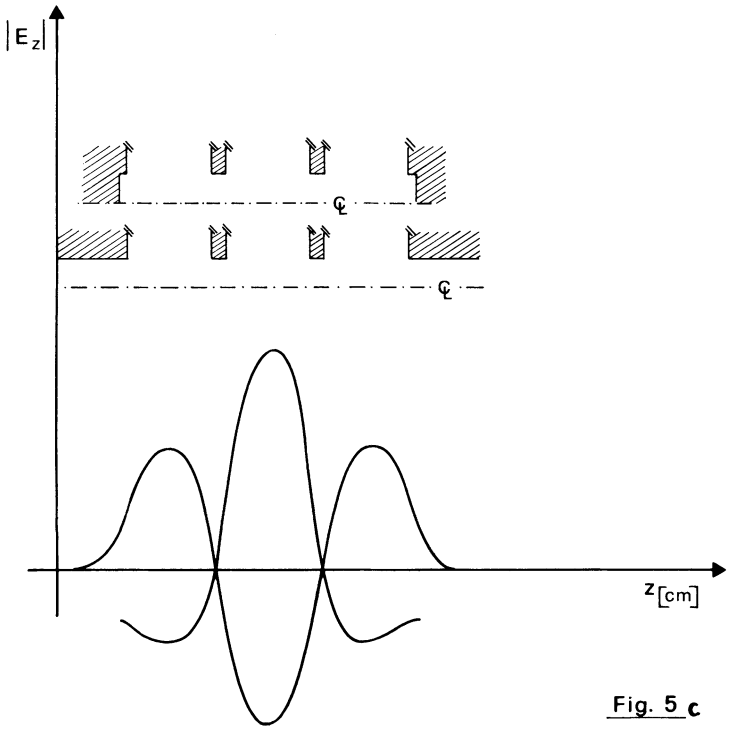

Fig. 5 c

Figure 5 (*Cont.*)

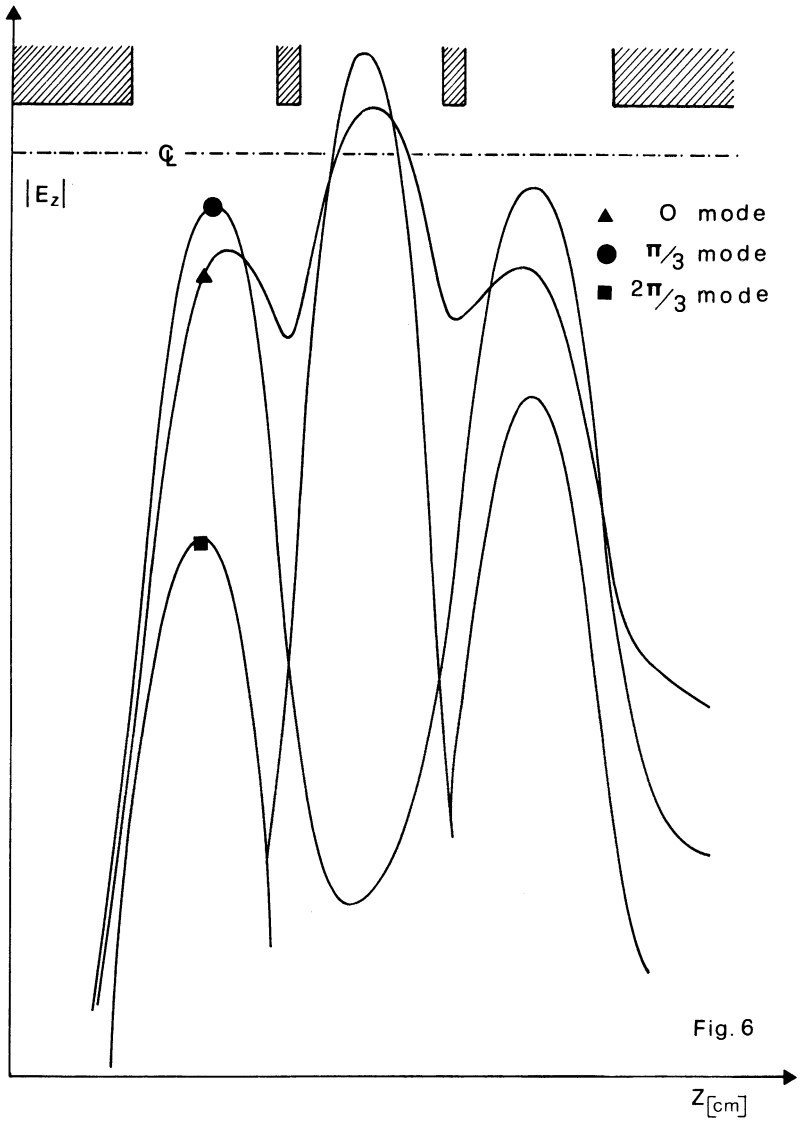

FIGURE 6 Measured axial electric field (absolute value) in a three-cell structure with beam tubes ($d/a = 2.25$): 0, $\pi/3$, $2\pi/3$ modes.

example these results for the same three-cell structure as in section 4 but with beam tubes ($d/a = 2.25$). In consideration of all the above, the approximation $C_B = \infty$ is a good one for a practical superconducting structure. Thence the theory of the previous section approximately holds and can still be used.

This is shown in a particular case by Fig. 7, which shows the electric-field distribution obtained by computer simulation of our three-cell structure with beam tubes compensated following the method of section 4.

It is not worthwhile to look for a better approximation of C_B, since in most cases the residual unflatness after compensation is not worse in structures with beam tubes than

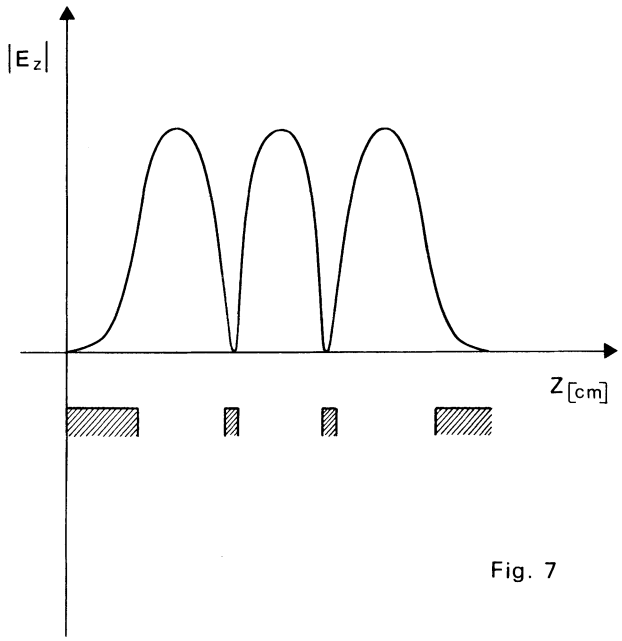

FIGURE 7 Computed axial electric field (absolute value) in the highest mode of a compensated three-cell structure with beam tubes ($d/a = 2.25$).

it is in structures terminated by metal plates and is comparable with the accuracy of LALAGE code.[13]

Since the working frequency of a practical structure may range from a few hundreds of megahertz (storage rings) to a few gigahertz (linacs) with a coupling coefficient of a few percent, the correction to the end cells range from a few tenths of millimeters to a few millimeters. The lower limit of this range is just the mechanical tolerance achievable by forming a niobium sheet against a die and then electron-beam welding together the resulting half cells, which is the standard procedure for superconducting structures. Thus it is worthwhile to use different cavities for end cells only for low-frequency structures. On the contrary, when dealing with higher-frequency structures it is better to make equal cells and carry out the compensation as a part of the tuning of the structure.

6. A PRACTICAL APPLICATION

The method developed in previous section has been successfully tested on a 4.5-GHz five-cell superconducting structure designed by us to be used as an accelerating device suitable for electrons of ultra-relativistic energy. Details on the design procedure of its elementary cell together with final shape and size can be found in a previous paper.[14]

Since computations by our method gave a 0.65% frequency compensation achievable by a 0.19-mm radius variation, we decided to build the structure with five equal cavities and to carry out compensation, together with tuning, by selective etching of the cells. Building of beam tubes was such that $d/a = 3.76$. Measurements on the uncompensated structure performed at room temperature by perturbation method[15]

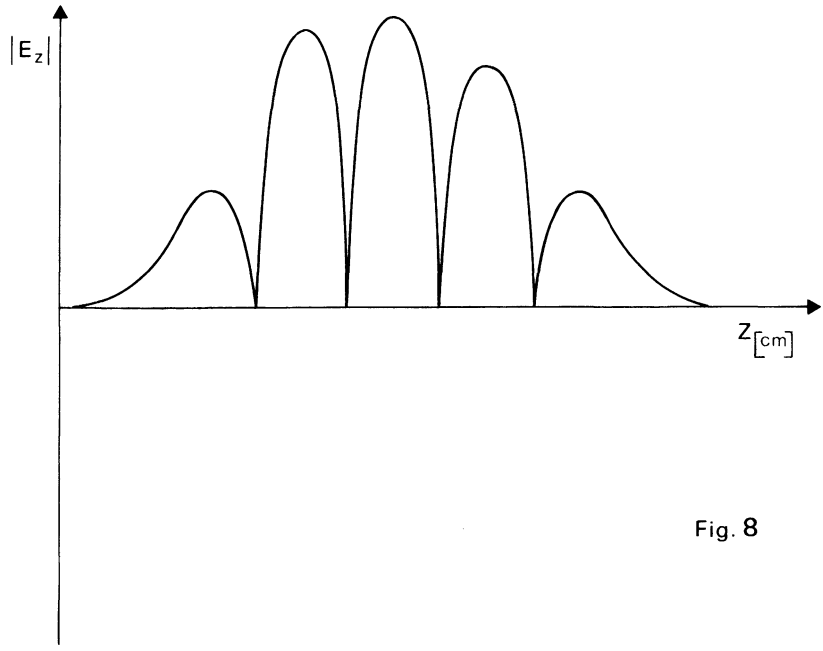

FIGURE 8 Measured axial electric field (absolute value) in the highest mode of the five-cell structure of Ref. 14 uncompensated.

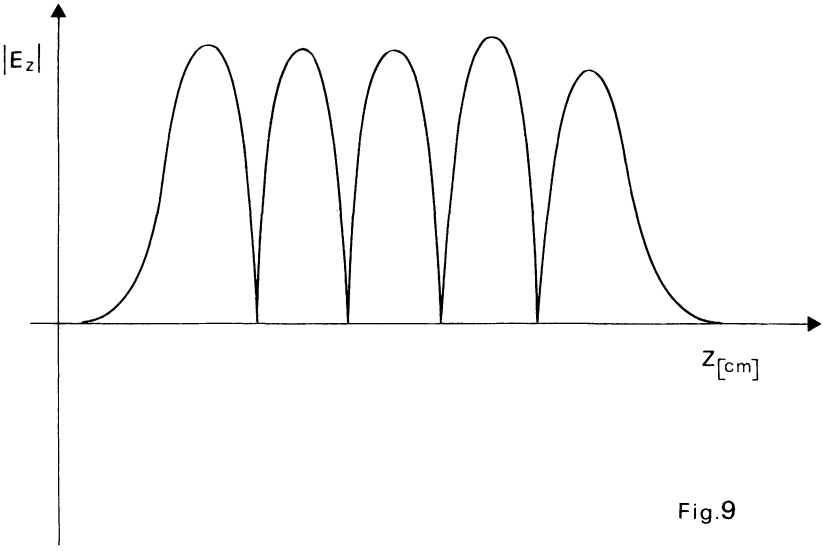

FIGURE 9 Measured axial electric field (absolute value) in the highest mode of the five-cell structure of Ref. 14 compensated.

TABLE II

Frequency corrections applied to each cell of the structure of Ref. 14 to obtain field flatness

Cell number	Total correction[a] $\Delta f/f$	−	Predicted correction $\Delta f_p/f$	=	Residual correction $\Delta f_R/f$
1	−3. %		0.		−3. %
2	−6.5%		−6.5%		0.
3	−8.5%		−6.5%		−2. %
4	−9. %		−6.5%		−2.5%
5	0.		0.		0.

[a] Notice that $\frac{1}{f}\left(\frac{\Delta f_2{}^2 + \Delta f_3 + \Delta f_4}{3} - \frac{\Delta f_1 + \Delta f_2}{2}\right) = -6.5\%$

gave the axial electric field distribution shown in Fig. 8. From the peak intensities of the axial field we got, by a tuning method,[16] the total frequency corrections required for field flatness. After these corrections were made by individual etching of each cell, we again measured the axial electric field; the results are shown in Fig. 9 from which it can be seen that field flatness in the highest mode is achieved.

From Table II, showing the total corrections made to each cell, we can see that the difference between the average correction to the three central cells and the average correction to the two end cells is just the compensation which follows from our method. Moreover, if we subtract from the total corrections those predicted by the model the residual corrections can be explained, as expected, by fabrication tolerances, since a radius variation of 0.1 mm in our cavities causes a relative frequency shift of about 3.4%.

ACKNOWLEDGMENT

The authors would like to express their sincere thanks to Ph. Bernard, E. Haebel, and J. Tuckmantel of CERN for the very helpful discussion and useful suggestions.

REFERENCES

1. P. M. Lapostolle and A. L. Septier, *Linear Accelerators* (North Holland, Amsterdam, 1957).
2. J. Halbritter, K. F. K Primarbericht, 08.02.02.P06E, (1979).
3. P. Fernandes and R. Parodi, INFN/TC-81/6, (1981).
4. H. C. Hoyt, D. D. Simmonds, and W. F. Rich, *Rev. Sci. Instr.*, **37**, 755 (1966).
5. K. Halbach and R. F. Holsinger, *Particle Accelerators*, **7**, 213 (1976).
6. E. Haebel and J. Tuckmantel, CERN/EF/RF/81-5 (1981).
7. T. I. Smith, *Stanford report HEPL* 437, (1966).
8. D. E. Nagle, E. A. Knapp and B. C. Knapp, *Rev. Sci. Instr.*, **38**, 1583 (1967).
9. G. E. Lee-Whiting, Proc. 1968 Proton Linear Accelerator Conference, Brookhaven Report BNL-50120 (C-54), 471, (1968).
10. W. Bauer, K. F. K. Primarbericht, 08.02.03.P01F, (1979).
11. S. Ramo, J. R. Whinnery, and T. Van Duzer, *Fields and Waves in Communication Electronics* (Wiley, 1965) p. 407.
12. P. Fernandes, R. Parodi, and A. Siri, INFN/TC-80/3, (1980).
13. P. Fernandes and R. Parodi, *Particle Accelerators* **12**, 131, (1982).
14. P. Fernandes and R. Parodi, *Alta Frequenza L*, 143 (1981).
15. P. Bramham, *Stanford report HEPL* 639, (1970).
16. V. Lagomarsino, private communication.